ASIA TURBOMACHINERY & PUMP SYMPOSIUM
SINGAPORE | 22 – 25 FEBRUARY 2016
MARINA BAY SANDS

FOUR QUADRANT CENTRIFUGAL COMPRESSOR PERFORMANCE

Elisabetta Belardini
Senior Engineer
GE Oil & Gas
Florence, Italy

Elisabetta is Senior Engineer of Radial Turbo machinery Performance within the Advanced Technology. She is responsible of performance predictability and risk assessment of centrifugal compressors, stall investigation and modeling of system dynamics. Elisabetta, received a M.S. degree with honor in Mechanical Engineering in 1996, a Ph.D. in Energetics in 2000 from University of Florence in the unsteady CFD simulation of turbo machinery and joined GE in 2005.

Dante Tommaso Rubino
Engineering Manager
GE Oil & Gas
Florence, Italy

Dr. Tommaso Rubino is currently the Manager of the Radial Turbo machinery Aerodynamic Design and Performance within the Advanced Technology Division. His responsibilities include the aerodynamic design and the performance predictability of the GE Oil & Gas turbo-compressors and turbo-expanders product lines. Dr. Rubino joined GE in 2006 as Design Engineer in Centrifugal Compressor NPI team, and then he has been responsible of the aerodynamic design of new stage families for Centrifugal Compressors and Pumps. Mr. Rubino received a B.S. and M.S. degree in Mechanical Engineering in 2002 and a Ph.D. degree in Mechanical Engineering in 2006 from Politecnico of Bari, and he graduated with honors in the Diploma Course program at the von Karman Institute in 2002

Libero Tapinassi
Engineering Manager
GE Oil & Gas
Florence, Italy

Libero Tapinassi is currently the Manager of Turbomachinery Aerodynamics and Heat Transfer department of Advanced Technology Division. His responsibilities include the aero-thermal design activities related to the development of GE Oil&Gas turbomachinery product line. Mr. Tapinassi joined GE in 2003 as Design Engineer in Centrifugal Compressor NPI team, and then he has worked as Manager of Centrifugal Compressor Aerodynamic team supporting stage development and performance improvement programs. Mr. Tapinassi received a B.S. degree (Environmental Engineering, 2001) from the University of Florence in 2001.

Marco Pelella
Engineering Manager
GE Oil & Gas
Florence, Italy

Marco is Engineering Manager for System Operability of Centrifugal Compressor & Turbo expander Applications. His responsibilities include the definition of Process Control Philosophy and Dynamic Simulations. Mr. Pelella graduated in Mechanical Engineering at University of Naples, Italy in 1997. He joined GE in 1999 as Design Engineer of centrifugal compressors then moving to office Team Leader of integrally geared and pipeline compressors, then as centrifugal compressors design office Engineering Manager in Le Creusot, France and axial and centrifugal compressors design office Engineering Manager for LNG and Down Stream applications in Florene.

ABSTRACT

The characterization of the compressor behavior in all quadrants of performance map has acquired, in the last years, growing attention.

Two dedicated experimental campaigns have been performed to characterize fourth quadrant and second quadrant operation in terms of performance, pressure fluctuations and mechanical vibrations. Experimental campaigns allowed the acquisition of performance curves of a centrifugal compressor in deep choke up to reverse pressure and indicated a large region of safe operating conditions at low peripheral Mach number. In stable reverse flow, the trends of work coefficient and pressure ratio were acquired for a large range of flow rates together with the evolution of vibration and pressure fluctuation along the speed lines. Pressure ratio and absorbed power for the different modes of operation can be very important to simulate dynamic scenarios far from the steady state operation and size accordingly compressor protection equipment and predict accurately compressor startup torque from pressurized condition (Fourth Quadrant Operations). The main frequency content and amplitude of pressure variations within the flow field or the radial/axial vibrations at the bearings are important to estimate blade loading and possible presence of excitation frequencies in the system. In the reported experience the operating points characterized by stable reverse flow rates close to the nominal one in direct flow did not show features much

more critical than in standard conditions (Second quadrant operation) . This result may be hopefully used to reduce BOP in early design phase of system layout.

INTRODUCTION

The so called four quadrant operation can occur in both axial and centrifugal compressors if the direction of flow or the sign of the pressure difference across the compressor reverses. In normal working conditions, the operating point stays inside the classical portion of the performance map, with positive flow (from impeller inlet to outlet), compression ratio higher than unity and positive torque (rotor is absorbing power). In case of failures of some parts of the system, emergency operations such ESD or transient operating conditions in general flow rate, pressure difference between inlet and outlet sections or speed can assume opposite values. Under such conditions, both compressor equipment (in particular impeller blades) and all other system devices experience unusual loading levels. Shaft torque may reverse in case of negative rotation.

The term four quadrant operation is used to indicate all the possible operating condition of a rotating machine. Deep choke (fourth quadrant) and deep surge with reverse flow (second quadrant) represent important four quadrant operations. The first is characterized by direct flow and rotation but reverse pressure and is likely to occur during compressor start up. In deep choke unusual high mass flow is forced across the machine due to the high inlet pressure and axial thrust across bearings may overcome capacity. Second quadrant is characterized by direct speed and pressure with reverse flow: gas is driven backward by an overwhelming discharge pressure typical during ESD or valve failures causing unusual blade and equipment loading.

Fourth and second quadrant characteristics have been experimentally investigated for a centrifugal compressor stage and, after a brief introduction about the four quadrant operating map, the results are presented.

FOUR QUADRANT MAP

In normal working conditions the operating point stays inside the portion of the performance map called normal operating map delimited by the surge and choke lines.

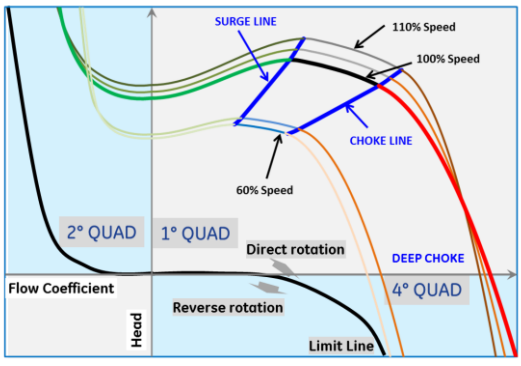

Figure 1 – Four Quadrant Compressor Map

Normal operating conditions are characterized by positive flow (from impeller inlet to outlet), compression ratio higher than unity and positive torque (rotor is absorbing power). Speed rotation is ranging from about 60% up to 110% of the nominal value (blue lines in figure 1). In transient operating conditions, flow rate, pressure ratio between inlet and outlet sections or speed can vary outside the normal operating map. Different areas can be identified in the four quadrant operating map of the compressor.

Deep Choke/Fourth quadrant: direct speed, direct flow, reverse pressure

In Figure 1, the area located on the right of the choke line is characterized by a pressure coefficient decreasing to zero (deep choke) or even negative values (4^{th} quadrant) for progressively increasing flow coefficients. Fourth quadrant is characterized by a downstream pressure lower or equal to the upstream, while speed rotation and flow are still in the same direction of design conditions. Deep choke area is likely to be entered by the compressor during start-up when one or more of last stages can operate in 4^{th} quadrant. The proper understanding of the basic physics at right of the choke line, in particular for power absorption is mainly important for the sizing of start-up devices.

Deep Surge/Second quadrant: direct speed, reverse flow, direct pressure

The area of the performance map on the left of the surge line in Figure 1 can be divided in two sections: the first is characterized by positive flow with positive slope in 1^{st} quadrant. This region is generally unstable considering the standard volumes involved in typical systems and the operating points reside in this region for very small periods of time. The second area (2^{nd} quadrant) is characterized by negative flow and negative slope in the pressure coefficient versus flow plane and is characterized by a stable behavior. This region is usually referred to as second quadrant, characterized by positive rotation, negative flow and positive speed. The physics of second quadrant is used for the simulation of ESD and the sizing of surge avoidance and control devices.

Reverse Rotation

During transient operations rotational speed can be inverted with respect to the design direction. Examples are present in literature and in the authors direct field experience. This situation may occur for instance during emergency stop of the train: in this situation the rotor is subject to extremely rapid deceleration reaching zero speed before the complete equalization of pressure. The residual pressure difference between compressor discharge and suction may accelerate the train in reverse rotation. Speed inversion can happen with both direct and reverse flow. The valve-like characteristic of the compressor at zero rotation and both positive and negative flow is called limit line and can be used to identify in performance map the positive and negative rotation regions. Experiments

have been not yet performed with reverse rotation and thus won't be addressed in this paper.

FOURTH QUADRANT EXPERIMENTAL DATA

Performance curves during standard validation tests are limited by the external characteristics of the closed test loop. In general, points at deep choke with low or negative values of pressure difference are not feasible.

The reliability of compressor performance is good up to the tested flow coefficient. Extrapolation capability above that point is generally poor: predictive tools (CFD or correlations based methods) suffer for the scarcity and inadequacy of validation data. Data are also generally lacking for the evaluation of pressure fluctuations or vibrations at flow rates above choke line. Possible consequences are represented by a too conservative operating range allowed to the compressor or inaccurate evaluation of power absorption during transients involving the knowledge of performance characteristics at deep choke (start-up).

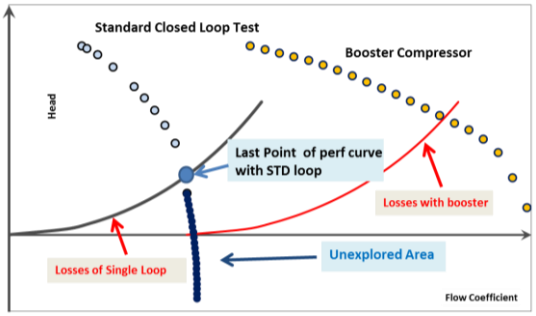

Figure 2 – Four quadrant test Arrangement

Acquisition of performance curves during standard testing is limited by the intersection with the loop characteristics (blue dot in Figure 2) and choke line is generally set close to this point. To extend safely the operating range a dedicated test arrangement has been designed in which a booster compressor has been connected in parallel with the tested stage. Booster compressor allows shifting the loop characteristics towards higher flow rates (from black to red line in Figure 2) and thus investigating the deep choke range. Besides it can provide a pressure gradient high enough to force the gas flow in the compressor and reach the full 4th quadrant range (Patent 249446). The test compressor is equipped with most advanced designed pipeline stage characterized by design flow coefficient of 0.03 and design impeller tip Mach number of 0.73.

Performance at choke

In Figure 3 and Figure 4 the measured performance in deep choke are reported for different reference tip Mach numbers. In particular the vertical red line represents the range which could be obtained using the classical model test loop arrangement: it can be noticed that due to the loop characteristics only a range of φ/φ_{Des} close to 1.6 could be explored. With the two parallel compressors arrangement shown in Figure 2, the additional curve range located to the right of the red line could be acquired. The rightmost points are limited by the maximum electrical power available for the booster compressor.

In Figure 3b the head and efficiency curves in first and fourth quadrant are reported for the tested compressor.

Both head and efficiency curves for the speed line corresponding to 68% of the design Mach number maintain smooth shapes for a large range of flow coefficients: last acquired point is characterized by a flow coefficient of 2.4 times the design value. The point of zero head/efficiency (equalization point) has been measured at a flow coefficient of almost two times the design one. Points with higher flow rates are characterized by a downstream pressure lower than upstream while the flow is partly powered by the booster compressor. Negative efficiency and head of the last point are about -22 and -1.25 times the corresponding design values.

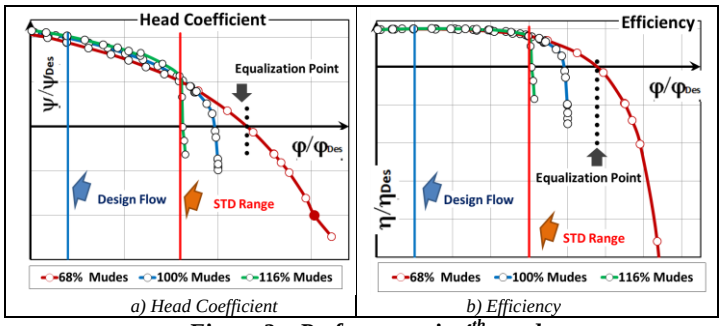

a) Head Coefficient *b) Efficiency*

Figure 3 – Performance in 4th quadrant

For design and 116% Mach numbers the curves of Figure 3 shows a choke limit due to the sonic throat reached at impeller inlet. In Figure 4b the Mach number contours obtained from CFD simulations are reported, indicating the presence of a shock wave close to the leading edge. In these cases the increase of flow coefficient beyond choke line is limited, also in presence of booster compressor. Negative values of efficiency and head have been anyway acquired in 4th quadrant up the maximum amount allowed by the electric motor.

The work coefficient trends are shown in Figure 4a: the speed line corresponding to 68% of the design Mach number confirms the regular and monotonic trend shown by head and efficiency curves of Figure 3. The work coefficient of the last point acquired has reduced to approximately 5% of the design value.

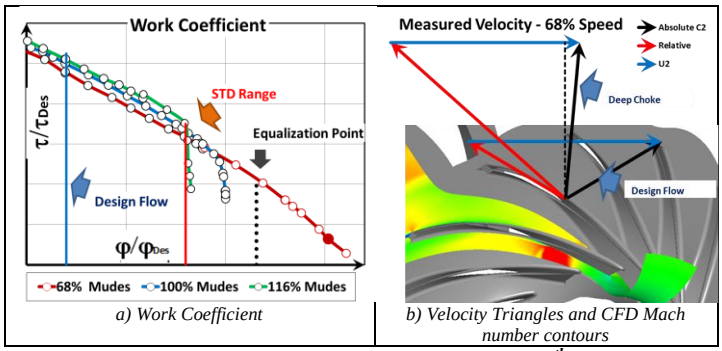

a) Work Coefficient *b) Velocity Triangles and CFD Mach number contours*

Figure 4 – Work Coefficient and velocity in 4th quadrant

Important outcome from this plot is that negative or zero work coefficients is not measured in realistic ranges of flow coefficient indicating positive power absorption: when pressure difference between inlet and outlet of the impeller is equal to zero (dotted black line in Figure 4a) compressor is still requiring power to maintain rotation. For this flow rate the measured work coefficient is around 0.4 times the design value. This value serves as a reference for magnitude of power to be provided at start-up of the machine (typically with zero pressure gradients across the compressor).

For design and 116% Mach numbers positive values of work coefficient are measured for all points acquired up and above the sonic throat limit.

In Figure 4b the measured velocity triangles at impeller outlet are reported for two operating point of the 68% speed line: the first one is close to the design flow coefficient while the other corresponds to one of the rightmost points acquired in the fourth quadrant campaign (brown dot in Figure 4a). As can be noticed with highest flow rate the relative flow angle (red arrows) measured at the outlet of the impeller is more radially inclined (about 10 degrees). The absolute flow angle at impeller outlet suits very close to the radial direction but the contribution to the work coefficient $\tau = (C_{t2}U_2 - C_{t1}U_1)/U_2^2$ is still positive. This is coherent with the almost zero work coefficient measured.

Negative values of work coefficient have been reported for axial compressors even with relatively smaller flow rates (above 1.20 the nominal flow according to Bammert et Al. and Gill) at which a turbine like behavior have been documented. In present case the value of work coefficient remains positive up to flow coefficients of the order of 2.5 times the design load. This behavior is mainly related to the typical axial direction of the flow at impeller inlet in centrifugal compressor stages, for which the contribution of $C_{t1}U_1$ is negligible in the expression of τ. In axial machines the tangential component of inlet velocity is generally significant and gives an important negative contribution in the work balance. This component can prevail at relatively low flow rates, often before the point of pressure equalization.

Vibrations and Fluctuations at choke

The trend of dynamic pressure are recorded during the 4th quadrant test campaign using 3 dynamic pressure sensors located inside the flow path at both impeller and vaneless diffuser outlet. In Figure 5 the frequency content of pressure pulsations in 4th quadrant range are compared with those of the design conditions for the lower Mach speed lines (68% of the design). In the small graphs the amplitude of pressure fluctuation at impeller outlet, divided by the average value, is plotted versus the frequency divided the 1xREV. At choke line the dominant frequency is represented as usual by the BPF=15xREV, caused by the passage of the 15 impeller blades at diffuser inlet, together with its second harmonics. The amplitude of the 2xBPF remains quite small: the range is around 1.5% of the average pressure at impeller outlet due to the limited loading of this operating condition. Considering points beyond the equalization point the 1xBPF becomes the dominant frequency. Besides the amplitudes of both BPF and 2xBPF increase: this is coherent with the increase of average dynamic pressure with the mass flow. Anyway the level remains inside the same order of magnitude: 3% is the maximum value measured for value 2.32 times the nominal flow rate.

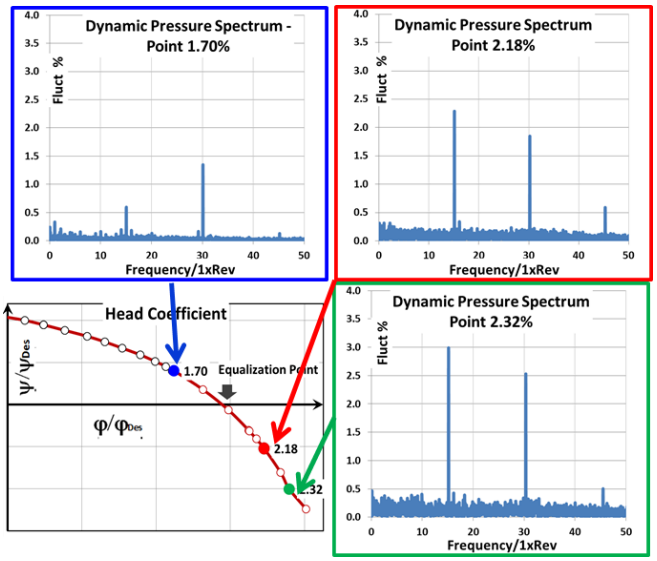

Figure 5 – Pressure fluctuations at low Mach

Axial and radial vibrations at bearings were recorded using standard commercial sensors. In Figure 6 the frequency content of radial vibrations is shown for the same three points considered in Figure 5. Vibrations in microns are plotted versus frequency. At choke line the dominant frequency is 1xREV together with the second harmonics. The amplitude is about 14 microns and the value remains almost unaffected up to deep 4th quadrant.

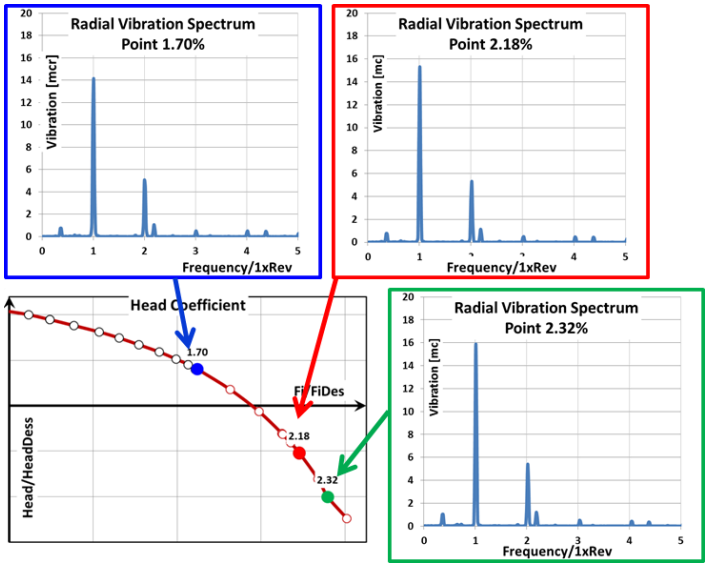

Figure 6 – Radial Vibration at bearings

In Figure 7 the frequency content of the dynamic pressure signal is shown for three points of the speed line at tip Mach number equal to 116% of the design value. Corresponding plots of vibrations are omitted since no different physics could be found with respect to the lower Mach number. The measured dominant frequency measured by dynamic sensors close to the choke line is the 1xBPF together with the second harmonics.

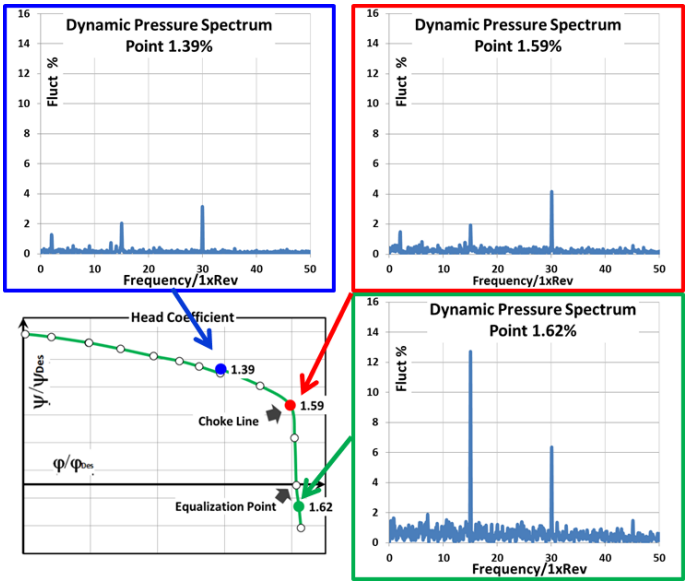

Figure 7 – Pressure fluctuations at 116% tip Mach number

The amplitude is about 4% of the average pressure at impeller outlet, higher than the value of 2% found for the speed line at 68% design (Figure 5) but with the same order of magnitude. After the development of the shock wave at impeller inlet, when the mass flow is about 1.59 the design value, the amplitude of pressure fluctuations rapidly increases reaching a value of 12% when the head is slightly below zero.

The comparison between the situations shown in Figure 5 and Figure 7 indicates that operating beyond the choke line or in the fourth quadrant can have a different impact on both compressor and system layout depending on the presence of shock waves in the flow path. In the absence of shocks the entity of pressure fluctuations and vibrations are not substantially different between the operation in deep choke and design conditions. Large flow rates can be reached, without causing important changes in the amplitude and frequency content of both pressure fluctuations inside flow path and vibration transmitted to the system. No different modes are expected to be excited with respect to the design conditions and the compressor is likely to be quite safely operated up to large flow rates. When a sonic throat is developed due to the combination of both high rotational speed and flow rate, the level of pressure fluctuations rapidly increases as also the amplitude of many frequencies. More excitation frequencies may be present, causing limitations in the time the machine can remain in a certain operating point.

The level of pressure fluctuation shown at different tip Mach numbers together with the extended performance curves can be used for a more accurate setting of the choke line and increase safely the operating range of the low Mach number operating machine in demanding application (parallel and series configurations etc…). According to the present design criteria, the choke line is conventionally located along a speed line when specified efficiency decay is measured with respect to the design point (indicatively between 0.10 and 0.30). This criterion may be too conservative in terms of allowable operating range in low Mach applications where no remarkable changes in flow features have been detected up to values of efficiency far below zero.

SECOND QUADRANT EXPERIMENTAL DATA

The 2nd quadrant flow is characterized by positive rotation, positive pressure but negative flow: it can occur when the pressure difference applied by system becomes larger than that provided by the compressor and flow is forced in reverse direction. This behavior can occur intermittently during surge cycles or continuously as result of system accidents or fast ESD with low inertia machines. Second quadrant behavior has been characterized using the same experimental scheme represented in Figure 2. In this case the booster compressor is forcing the flow to be stable in reverse flow. The instrumentation (Kulite, thermocouples and Kiel probes) has been rotated according to the different expected flow direction. In the 2nd quadrant work coefficient τ_{Sec} and pressure ratio r_{Sec} are computed and plotted according to the following conventions (Belardini et Al 2015):

$$\tau_{Sec} = \frac{H_{0Out} - H_{0Inlet}}{u_2^2} \quad \textbf{Eq.1}$$

$$r_{Sec} = \frac{P_{0Inlet}}{P_{0Out}} \quad \textbf{Eq.2}$$

$$\varphi = \frac{4\dot{m}}{\rho_{0inlet}\pi D_2^2 u_2}$$

In **Eq.1** and **Eq.2** H_{0Out} and H_{0Inlet} are the values of total enthalpy of the gas at the outlet and inlet from compressor respectively: work coefficient is positive since power is transmitted to the flow increasing the energy content $H_{0Out} > H_{0Inlet}$. The terms P_{0out} and P_{0Inlet} are the corresponding values of total pressure in the outlet and inlet: pressure ratio is typically higher than unity due to the high losses inside the flow path during flow reversal $P_{0Out} < P_{0Inlet}$. This definition allows more consistent comparisons amongst 1st, 2nd and 4th quadrants. The flow coefficient in the second quadrant is referred to the total density at impeller outlet diameter which is the inlet section in reverse flow and is considered as negative. Angles are measured from radial direction.

Performance in 2nd quadrant

The trends of τ_{Sec} and r_{Sec} measured in the second quadrant are reported in Figure 8 as a function of flow coefficient. At the lower tip Mach number (68% of the design speed), when the negative flow is equal to the design flow coefficient, the pressure ratio across the compressor is quite

similar to the one experienced in direct flow. Reducing the amount of reverse flow to zero, pressure ratio tends to a limit value: the limit pressure ratio is corresponding to centrifugal forces at the imposed rotational speed. Increasing reverse flow above nominal value, pressure ratio increases regularly; no choke is detected in the curve. For design speed line (100%) the limit pressure ratio consistently increases with the square of the speed and the slope of the curve is steeper due to the quadratic relation of losses with the higher velocities involved. A limiting flow is reached, after which an abrupt drop in pressure ratio is experienced. This seems related to the blocking of impeller inlet section at approximately 90% of design flow: the gas is continuously accelerating in the return channel, the diffuser and impeller reaching maximum velocity in the outlet. Same considerations can be drawn for the curve corresponding to 116% of the design Mach number.

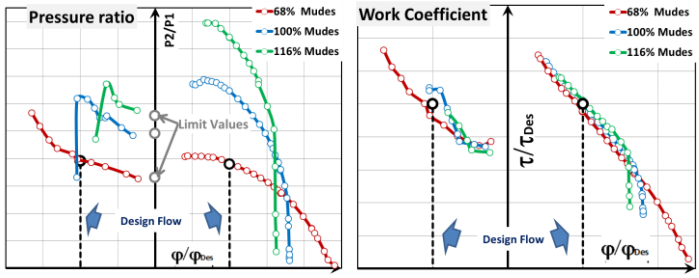

a) Pressure ratio *b) Work Coefficient*

Figure 8 –Measured Performance 2nd quadrant

The shape total-to-static pressure characteristic for this mode of operation is similar to that found by Gamache and Greitzer [1990] for an axial compressor stage. Only difference is represented by the higher discontinuity exhibited for low negative flow coefficients near the y-axis. This may be related to the relevant role played in a radial machine by centrifugal forces.

The work coefficient characteristic in the second quadrant is shown in Figure 8b and is computed as the ratio between enthalpy increase between impeller inlet and outlet, divided by velocity squared at impeller outer diameter (**Eq.1**). The sign is positive, since power is provided by the driver to maintain rotation, even if the mass flow is driven by the pressure difference of the system. In fact a higher total temperature of the flow is measured when leaving the impeller at the classical inlet section. At low Mach number and with a negative design flow, the work coefficient is close to the design value. It decreases towards a minimum value and then seems to slightly increase again towards zero flow rates. The stability limits of the system could not allow acquiring points closer to the y-axis to measure the limit of work coefficient at zero flow. An upgrade of the test rig is under evaluation to repeat the test in negative unstable range with dynamic acquisition of both mass flow and pressure. In any case the missing region is likely characterized by positive slope and thus unstable behavior: time spent in this zone is not expected to be influent in dynamic simulations. The increase in work coefficient close to zero flow has not been completely understood from a physical point of view. A simple 1D evaluation based on velocity triangles leads to a limit value of the work coefficient equal to the ratio between inlet and outlet diameter square $\tau_{Lim} = (D_1/D_2)^2$. This value corresponds to the work done by centrifugal forces at a given rotational speed. From experiments it looks like that, in real environment, other sources of power absorption are realistically present, which are particularly evident with low flow: friction, ventilation, etc…. CFD computation is ongoing to deepen the understanding of flow field structures at reverse flow.

Velocity triangle with reverse flow

Flow direction is measured by 3-hole probes located at both impeller inlet and outlet: the same probes used in direct flow have been retained, but aligned to the new expected directions: the blade angle at return channel inlet and the blade angle at impeller inlet (in direct flow).

In Figure 9a three velocity triangles at impeller outer diameter are reported: one in first quadrant and two in 2nd quadrant at minimum and maximum measured flow coefficients of the 100% speed line. In direct flow, close to design condition, outlet relative velocity (red arrow) is aligned with the impeller blade angle. The absolute velocity is obtained adding the contribution of tip speed and is represented by the black arrow. The inlet vane angle of the downstream return channel has been aligned to this direction: in 2nd quadrant the experimental absolute flow angle is in first approximation aligned with this direction for both design and off-design flow rates (Belardini et Al). The relative velocity can be computed adding rotation speed and is characterized by a very large incidence angle with the impeller trailing edge (around 130°). Since the trailing-edge is relatively sharp, the flow is expected to generate a large separation zone within the impeller vane passage before aligning to the blade surface, causing high incidence losses causing the trends of total pressure discussed in Figure 8.

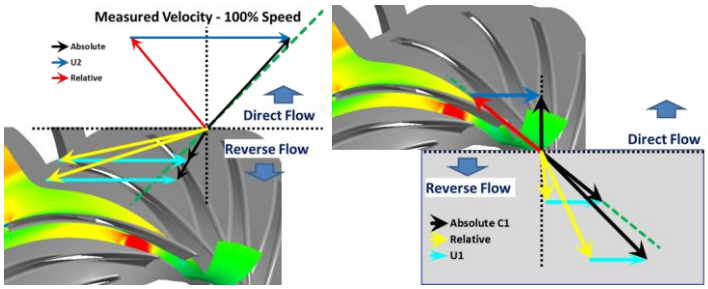

a) Impeller Outer Diameter *b) Impeller Inner Diameter*

Figure 9 – Measured velocity triangles in 2nd quadrant

In Figure 9b the measured velocity triangles at impeller inner diameter are reported for the same points of In Figure 9a. In 2nd quadrant absolute velocity vectors are approximately aligned to the geometrical blade angle. Considering the contribution of peripheral speed the direction of relative flow leaving the impeller has a strong component opposite to the rotation speed with respect to the leading edge. The deviation

increases when the mass flow reduces: at very low flow rates the relative velocity is practically aligned with the radial direction. The 1D model based on velocity triangles computes the work coefficient in 2nd quadrant supposing that the outlet relative velocity at impeller leading edge is aligned with the blade angle. The high deviation shown by experimental data indicate that this assumption leads to an overestimation of the work coefficient particularly evident with lowest flow.

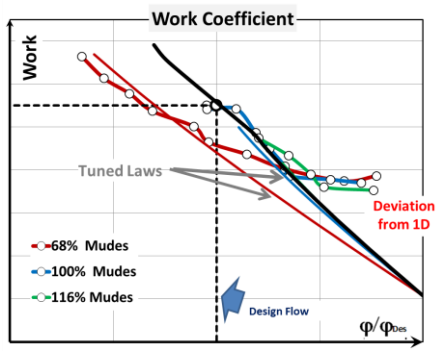

Figure 10 – Tuned work coefficient

In Figure 10, the black straight line represents the work coefficient computed assuming the relative velocity at impeller inlet is aligned with the blade angle. However this is not sensitive to the Mach number and seems poorly accurate for the lowest 68% speed line. A simple way to account experimental data is the introduction of a sort of deviation angle (equivalent to the slip factor in direct flow) directly tuned on experimental data. In Figure 10, the red straight line is obtained after the introduction of a deviation angle equal to the measured value: the accuracy of the work coefficient improves for large flow coefficient and the slope seems more accurately captured. The discrepancy at low reverse flow rates, between the computed and measured work coefficient, discussed in previous chapter, is not recovered. The presence of additional power absorption mechanisms, not related to velocity triangles and already mentioned in previous chapter seems confirmed.

Pulsations & Vibrations in 2nd quadrant

In Figure 11, stall coefficient C_{Stall} at impeller outlet is reported for different values of reverse flow rate. The stall coefficient is defined as the ratio between the RMS of the amplitude of sub-synchronous pressure fluctuations $\tilde{p}_{SubRMS}$ and average dynamic pressure at impeller outlet $0.5\overline{\varrho}\overline{V}_2^2$:

$$C_{Stall} = \frac{\tilde{p}_{SubRMS}}{0.5\overline{\varrho}\overline{V}_2^2}$$

This parameter is used as an indication of the presence of rotating stall or other unsteady phenomena at impeller or static parts location. When no stall is present the main frequency content is represented by the blade passing frequency and its harmonics. In general the value of the stall coefficient when the stage is operated close to the design conditions is in the order of 0.1 and rapidly increases in presence of rotating stall, reaching and sometimes overcoming unity. In 2nd quadrant, the level of the stall coefficient is close to the standard values measured in direct flow up to about 85% of the design flow. This flow is close to the point where the trend of the work coefficient starts departing from the linear trend and predictability of 1D model decreases. Besides, the relative velocity angle is impacting the blades very close to the leading edge were blade curvature may reflect back the flow. Further decreasing flow coefficients below 85%, the stage performance parameters are globally stable, but the amplitude of the stall coefficient increases rapidly up to values in the order of 3.8. Pressure fluctuations are almost 4 times the average dynamic pressure of the section.

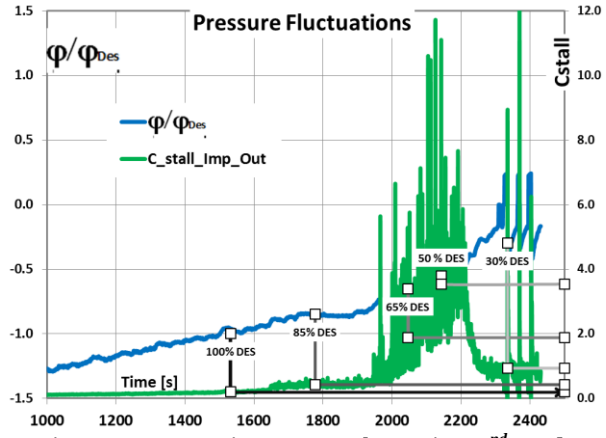

Figure 11 – Dynamic Pressure Fluctuations 2nd quadrant

The phenomena can be followed qualitatively in the waterfall diagram (Figure 12), where a complete span of the 2nd quadrant operating range is fulfilled and the starting of the unsteady path is detectable. The energy associated with these unstable phenomena reaches a maximum at around 50% of the design flow and then decreases for very low flow rates. In Figure 13 the amplitude of pressure fluctuations is reported at 100%, 50% and 30% flow rates. The frequency of the unsteady path is around 1.5 the frequency of rotation, being its nature to be completely understood.

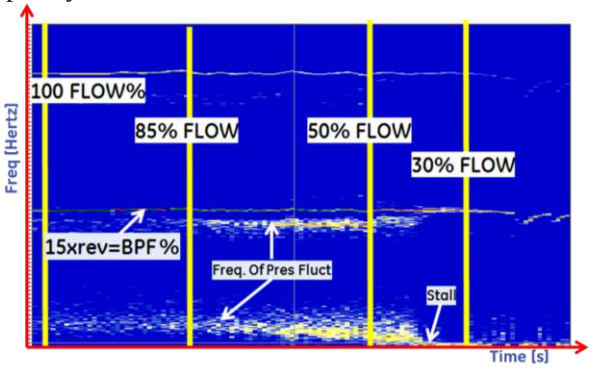

Figure 12 – Dynamic Pressure – Waterfall Diagram

A more clear rotating sub synchronous phenomena can be detected at around 30% design flow with a frequency close to 20% of the rotational speed (see Figure 13). For lower flow coefficient a phenomenon similar to surge in direct flow is

detected with pressure pulsations propagating upstream and downstream the compressor. In Figure 14 the trends of axial and radial vibration are reported during the same time frame of pressure fluctuations shown in Figure 11 and Figure 12.

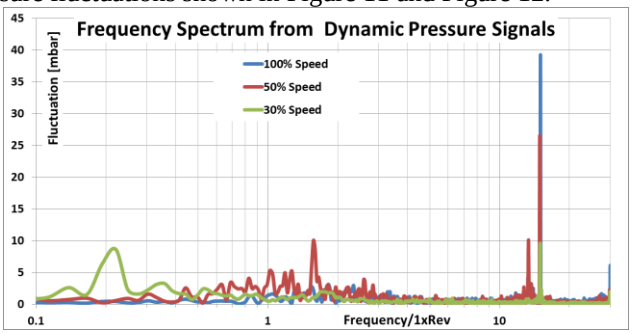

Figure 13 – Dynamic Pressure – Frequency Content

An increase of axial vibrations can be detected when dynamic pressure probes start measuring high levels of pressure fluctuations. Instead no perturbation of radial vibration level can be associated to the same fluctuations Present experimental campaign in 2nd quadrant indicated that both work coefficient and pressure ratio can be computed using the simple 1D approach but a high level of accuracy can be obtained provided that some experimental based correlation is given for deviation angle and losses. For lower reverse flow the experiments indicated the presence of pressure fluctuations associated with an increase of axial vibration and a deviation of power absorption from the linear behavior. The nature of the phenomena requires a further deeper investigation with advanced predictive tools such unsteady CFD or more dedicated experimental campaigns.

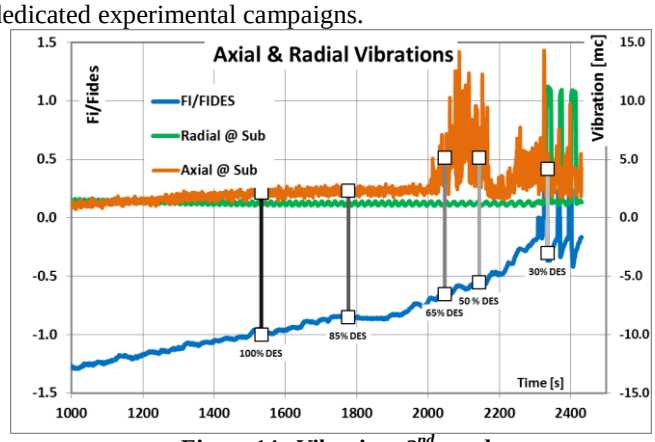

Figure 14 –Vibrations 2nd quadrant

CONCLUSIONS

In this paper the experimental investigation of large operating range of a centrifugal compressor are reported. These modes of operation are outside the standard operating conditions of the machine but the knowledge of basic features of performance parameters and vibration is important for a better sizing and verification of start-up equipment or anti surge devices. In this regard, the first main outcome of present experimental campaigns is represented by the quite safe operating conditions in deep choke and fourth quadrant operating range provided that the rotating speed of the machine is sufficiently low to avoid sonic regions in the flow path.

On the other side, present experience showed that when machine is operated in the stable reverse flow condition, pressure fluctuations and vibration are higher with respect to the values measured in nominal direct flow operating conditions, but not dramatically. This result may allow simplifying the design of system layout: in particular when during ESD in the worst scenario, no surging cycle is expected but only a reverse flow sustained steadily by the system (which is actually the most typical experience), the additional ASV's, such as hot or cold gas by-pass valves, may be reduced in size or eventually removed optimizing the Plant BOP.

At moment these results are encouraging but related to a single experience. In the future, same experience will be repeated on different types of compressor stages and operating conditions to assess the generality of present conclusions. From a modeling point of view at date, a simple one dimensional approach based on velocity triangle has been used to reproduce the experimental data. This model has shown some limitations to capture flow behavior, especially at low reverse flow rates where some more complex power absorbing mechanism has been clearly shown by experiments. This phenomenon seems connected with the development of unsteady fluctuations at impeller inlet preventing the simple 1D analysis to be accurate enough. However, both better understanding and further experimental confirmation are essential. In this regard a full CFD unsteady computation could help a better explaining or understanding of the phenomenon, allowing deeper insight of the flow structures present at impeller outlet.

NOMENCLATURE

(all variables are in italics)

u	= Impeller tip speed	(m/s)
H	= Entalphy	(J/kg)
r	= Pressure ratio	(-)
τ	= Work coefficient	(-)
φ	= Flow coefficient	(-)
ρ	= Density	(kg/m^3)
$\dot{m}$	= Flow Rate	(kg/s)
D_2	= Impeller tip diameter	(m)
D_1	= Impeller inner diameter	(m)
M_u	= Impeller tip Mach number	(-)
η_p	= Polytrophic efficiency	(-)

(acronyms used)

ESD	= Emergency Shut Down
BOP	= Balance of Plant
CFD	= Computational Fluid Dynamics
RMS	= Root Mean Square
1xREV	= Frequency corresponding to rotational speed
BPF	= Blade Passing Frequency
ASV	=Anti Surge Valve

(subscripts used)

Sec	= Second quadrante

Des =Design

REFERENCES

Bammert, K., Zehner, P.” Measurements of the Performance of an Air Turbine Stage at Positive and Negative Mass Flow and Rotational Speed (Four-Quadrant Characteristics)”, Journal of Engineering for Power JANUARY 1978

Gill,A., “Four Quadrant Axial Flow Compressor Performance”, Phd Thesis 2011, Stellenbosch University

Belardini, E., Rubino, D. T., Tapinassi, L., Pelella, M., “Modeling of Pressure Dynamics During Surge and ESD”, 3rd Middle East Turbomachinery Symposium (METS III-February 2015)

ACKNOWLEDGEMENTS

The authors would like to thank GE Oil & Gas for permission to publish this paper and all colleagues from OGTL laboratory for the support in the arrangement of the rig, the design and installation of special instrumentation, test execution, post processing of data as also the helpful support in the interpretation.